1. DRAG MEASUREMENTS FROM DIFFERENT WIND TUNNELS

By Ralph P. Bielat, Arvo A. Luoma,
NASA Langley Research Center

and James C. Daugherty
NASA Ames Research Center

SUMMARY

This paper examines the question: How good a correlation can be obtained from drag measurements made in different wind-tunnel facilities? The correlations considered pertain only to drag data which were obtained on the same models from investigations in various wind tunnels where special efforts were made to duplicate the exact test conditions.

Drag data obtained for the same model in different wind tunnels at subsonic, transonic, and supersonic speeds agreed within 3 percent, provided the tests were made in accordance with the rules and techniques developed for wind-tunnel tests at these speeds. In the application of these rules and techniques, proper consideration must be given to model support systems, transition strips, tunnel wall effects, test limitations, and so forth. Large-scale models, which permit high values of model Reynolds numbers, can be tested at subsonic speeds in relatively small transonic tunnels, and a high level of confidence can be placed in the results of such tests. Good correlation exists between model data obtained in the wind tunnel and by the rocket technique where the tunnel constraints are not present.

INTRODUCTION

An accurate assessment of the drag characteristics is essential in the design of a new airplane. To a large extent, this assessment is based upon the results of extensive wind-tunnel investigations of scaled models of the airplane. Because the conception of the airplane is relatively fluid during the early design stages, the wind-tunnel models of the airplane will usually differ in numerous details, and often in scale, from each other and will invariably differ from the "final" conception of the airplane. The correlation of the drag data of such models, consequently, can become a difficult problem, particularly when the tests are made in different tunnels. Unsatisfactory correlation in drag measurements often can be reconciled when proper consideration is given to differences in models, test conditions, test techniques, test limitations, data acquisition, data accuracy, data corrections, and so forth.

This paper examines the question: How good a correlation can be obtained from drag measurements made in different wind-tunnel facilities? The correlations considered pertain only to drag data which were obtained on the same models from investigations in various wind tunnels where special efforts were made to duplicate the exact test conditions. First, some of the testing techniques required to obtain reliable aerodynamic data at transonic speeds are discussed, and then comparisons of the experimental drag measurements from different transonic wind tunnels are shown. Second, some of the problems associated with testing large models at subsonic speeds in a transonic wind tunnel are considered, and then some experimental results from two transonic tunnels are compared. Third, data obtained in the wind tunnel are compared with data obtained by the rocket technique on an identical model. Last, tests conducted at supersonic speeds are discussed and then comparative data from different tunnels are presented. No attempt is made in this paper to correlate wind-tunnel results with full-scale flight results or to extend wind-tunnel results to full-scale Reynolds numbers.

SYMBOLS

c	chord of airfoil section, in.
C_D	drag coefficient
ΔC_D	rise in drag coefficient above minimum value
$\frac{\Delta C_D}{(\Delta C_L)^2}$	drag-rise factor
$C_{D,b}$	base drag coefficient
$C_{D,min}$	minimum value of drag coefficient
C_L	lift coefficient
ΔC_L	change in lift coefficient from value corresponding to minimum drag coefficient
l_s	axial distance required for model nose shock to traverse the supersonic flow to test-section boundary and reflect back to test-section center line, in.
M	Mach number
R	Reynolds number

t maximum thickness of airfoil section, in.

x axial distance from model base to mean location of tunnel normal shock, in.

α angle of attack, deg

Λ sweep angle of wing, deg

DISCUSSION

Testing Techniques at Transonic Speeds

Model size in relation to tunnel size is one of the critical problems to be considered when testing at transonic and supersonic speeds; the significance of this relationship is illustrated in figure 1. In order to assure interference-free data, the model must be sufficiently short to avoid impingement of boundary-reflected disturbances from the tunnel walls on the model, or even close to the base of the model, as indicated by the schematic drawing in the figure. In figure 1 the approximate shock-reflection distance l_s in inches is plotted against free-stream Mach number for airplane-type configurations for three NASA tunnels differing in size. The shock-reflection distances for the Langley 8-foot transonic pressure tunnel were experimentally determined for a wing-body model of high fineness ratio. A discussion of the Langley 8-foot transonic pressure tunnel results, including the applicability of the results to other models differing in size or shape, is given in reference 1. The approximate shock-reflection distances shown in the figure for the other two tunnels are estimates based on the Langley 8-foot transonic pressure tunnel results and the relative sizes of the tunnels.

The primary purpose of this figure is to illustrate the fact, which is well known to transonic and supersonic wind-tunnel engineers, that when the same model is tested in a larger wind tunnel interference-free data can be obtained at lower supersonic Mach numbers. As an example, an investigation was made in the Langley 8-foot transonic pressure tunnel on a 43-inch-long model, and it was found that a supersonic Mach number of 1.2 was required before interference-free supersonic data were obtained. Figure 1 indicates that tests of the same model in the larger wind tunnels would give interference-free data at a Mach number of approximately 1.1 in the Ames 11-foot transonic tunnel and approximately 1.07 in the Langley 16-foot transonic tunnel.

Each combination of test model and wind tunnel, however, offers a somewhat different problem with regard to the effects of boundary-reflected disturbances. Therefore, if a precise determination of the shock-reflection distances and the minimum supersonic Mach number for interference-free testing is needed for a specific model in a given wind tunnel, then actual experimental interference studies are necessary at the supersonic Mach numbers.

Figure 2 illustrates the effects of boundary-reflected disturbances on drag when the same 43-inch-long model is tested in two different-size wind tunnels at Mach numbers less than the minimums shown in figure 1. Drag coefficient is plotted as a function of Mach number in figure 2. It should be pointed out that the zero for the drag scale has been suppressed in this figure and also in several of the figures to follow. Note that the effect of boundary-reflected disturbances on drag (affected test points shown by the solid symbols) extends over a substantially larger Mach number range in the smaller wind tunnel than in the larger wind tunnel. The solid symbols in the figure show data in a Mach number range in which data normally would not be obtained in either tunnel in tests of models of this size.

Figure 3 illustrates the problems associated with testing the model in the vicinity of the tunnel normal shock. (See ref. 2.) Shown plotted in this specific example is the drag coefficient as a function of the distance of the model base from the tunnel normal-shock position, where $x = 0$ represents the model base in the normal shock as indicated by the dashed model lines. These data are for a free-stream Mach number of 1.2. Although the data were obtained in a solid-throat tunnel, the general results are applicable to any transonic or supersonic tunnel. It is quite obvious that the positive pressures associated with the tunnel normal shock can produce very significant drag reductions as the base of the model approaches the shock location, and tests of the model generally should not be made under conditions where the data can be affected by the proximity of the tunnel normal shock.

Most models are supported by stings in the wind tunnel. Such stings must be carefully designed if valid drag information is to be obtained, especially in transonic testing. A general recommendation for transonic testing is a sting which has a small ratio of sting diameter to model-base diameter, which has a constant-diameter section approximately 5 model-base diameters long, and which has a sting flare angle (total) no greater than approximately 6°. Some insight into the nature and magnitude of sting interference can be found in references 3 to 7.

Some specific examples of the effects of support interference at transonic speeds other than the interference caused by the usual sting supports will now be discussed. Figure 4 illustrates the effect of support-strut interference on the drag coefficient of a missile configuration at 0° angle of attack. (See ref. 8.) The strut was used to stiffen the sting in a lateral plane, especially at angle of attack. The strut had a chord of 3 inches and a thickness ratio of 21 percent, and was located 4 base diameters downstream of the model. The upper curves represent the total drag coefficient and the lower curves represent the forebody drag coefficient. The drag coefficients for this figure are based on body cross-sectional area. These data show that the presence of the strut caused reductions in the total drag coefficient, especially near $M = 1.0$. However, these reductions in the drag coefficient are due only to increases in the base pressure caused by the presence of the strut, since the forebody drag coefficients are unaffected by the presence of the strut.

Figure 5 illustrates the effect of support interference on drag for an airplane configuration which has both base and boattailing areas subject to the

influence of the pressure field of the support. The upper sketch shows an auxiliary support system which was used to obtain combined pitch and sideslip angles of the model. The middle sketch schematically illustrates a mockup of the above auxiliary support system. This mockup consisted of a dummy support, as shown. Tests were made with the dummy support on and off (as indicated by the middle and bottom sketches) in order to determine the interference of the auxiliary support. Minimum drag coefficient is plotted as a function of Mach number; in this case, the drag has not been corrected for base drag. Note the drag reductions for Mach numbers less than 1.2, and particularly the large reductions at speeds near sonic, caused by the positive pressure field with the dummy support on. Figure 6 shows the same comparison as in figure 5 except that in this case the minimum drag values have been corrected for base drag. Again note the effect of the dummy support on the drag. The drag reduction is less than that shown in figure 5, but it is still substantial near a Mach number of 1.0 because of the model boattailing.

Models and Test Conditions for Comparisons

Some of the drag measurements from different wind-tunnel facilities are compared next. In each of the comparisons, the same physical model was tested in two or more wind tunnels, and usually the same sting and the same internal balance were used. In each comparison the model was tested in the different wind tunnels at the same test conditions, except in one or two cases where the Reynolds numbers were somewhat different. Transition was fixed according to the methods described in reference 9 in order to insure a turbulent boundary layer on the models. A discussion of the use of grit-type boundary-layer transition strips on wind-tunnel models is given by Braslow, Hicks, and Harris in paper no. 2.

Comparisons at Transonic Speeds

The first of the comparisons shows the variation of the minimum drag coefficient with Mach number for a variable-sweep configuration (fig. 7). Sweep angles of 26° and 72.5° are shown. Air flowed through the ducts, and the drag has been corrected for the internal drag as well as for the base drag so that the drag coefficient is the minimum net external drag. The tests were conducted in three NASA facilities: the Ames 11-foot transonic tunnel and the Langley 8-foot and 16-foot transonic tunnels. The data shown are for a constant Reynolds number of 2.5×10^6 per foot. The data from the Langley 16-foot transonic tunnel were obtained at somewhat different Reynolds numbers, however, and these data have been corrected for the difference in skin friction between the test Reynolds number and the constant Reynolds number value of 2.5×10^6 per foot. Attention is again called to the fact that the origin for the drag scale is not shown in the figure. Note the correlation which has been obtained in the three facilities throughout the Mach number range shown. For example, the spread in the faired curves amounts at most to about 5 counts of drag (where one count of drag is equivalent to a drag coefficient of 0.0001), or 2 to 3 percent, in the subsonic Mach number range and about 2 or 3 counts of drag, or 1 percent, at supersonic speeds.

Figure 8 shows the variation with Mach number of the minimum drag coefficient and figure 9 shows the drag-due-to-lift factor (for lift coefficients up to about 0.3) for two wing sweep angles for a V/STOL configuration. The wind-tunnel tests were made in the NASA Langley 8-foot transonic pressure tunnel (ref. 10) and in the National Aero- and Astronautical Research Institute (NLR) 6.55- by 5.25-foot subsonic-transonic pressure wind tunnel, Amsterdam, Netherlands. As with the previous model (fig. 7), air flowed through the ducts and the drag has been corrected for the internal drag and base drag. The Reynolds numbers in the two facilities were approximately the same. Again, note the correlation which exists in both the minimum drag coefficient and drag-due-to-lift factor in both facilities. At most, the difference in the drag data amounts to about 7 counts of drag, or 3 percent.

The data presented in figures 10 and 11 are for a delta-wing configuration. Figure 10 shows the minimum drag coefficient and figure 11 shows the drag-due-to-lift factor (for lift coefficients up to about 0.3) plotted against Mach number. The wind-tunnel tests were made in the NASA Langley 8-foot transonic pressure tunnel and in the Cornell Aeronautical Laboratory 8-foot transonic wind tunnel for a constant Reynolds number of 2.5×10^6 per foot. The maximum spread between the faired drag curves amounts to 4 counts of drag, or 3 percent.

Large Models at Subsonic Speeds

In wind-tunnel tests, a large model is desirable since the model Reynolds numbers will be higher. At transonic and supersonic speeds the model size is usually limited by the problem of boundary-reflected disturbances existing at Mach numbers greater than 1. This constraint on model size does not exist, of course, when the tests are to be made only at subsonic speeds. Since the wind tunnel with slotted or porous walls has greatly reduced or eliminated the solid-blockage interference, a substantially larger model can be used for subsonic tests in a transonic (slotted) wind tunnel than can be used for subsonic tests in a comparable closed-throat tunnel. However, the problem of the downwash due to the tunnel-boundary interference on the lift of a large model is still to be considered. This type of interference is a function of the cross-sectional shape of the tunnel; the type, distribution, and amount of tunnel wall ventilation; the ratio of wing span to tunnel width; the ratio of wing area to tunnel cross-sectional area; and the lift coefficient. A recent theoretical analysis of tunnel-boundary interference (ref. 11) includes calculations of the spanwise variation of the interference and the effect of sweepback. Theory indicates that for a large model in the Langley 8-foot transonic pressure tunnel, the interference of the tunnel walls on the average induced flow is small, with the spanwise variation from wing root to wing tip being approximately twice the average value.

Figures 12 and 13 show comparative drag data at high subsonic Mach numbers on the same 5-foot-span model of a large subsonic transport. The model was investigated in the Langley 8-foot transonic pressure tunnel and in the considerably larger Langley 16-foot transonic tunnel. The Reynolds number was the same in both tests. The drag and lift data shown are the mean results obtained from tests of the model upright and inverted. The data from both tunnels have been corrected for the internal drag of the four engines, for base drag, for

buoyancy, and for the average downwash due to the tunnel-boundary interference on lift. This interference at a lift coefficient of 0.5, for example, was estimated to be an average downflow to the model of only 0.05° in the Langley 8-foot transonic pressure tunnel and 0.01° in the Langley 16-foot transonic tunnel. The effect of the interference correction on drag coefficient at a lift coefficient of 0.5 was to reduce the drag coefficient by 0.0005 in the 8-foot tunnel tests and by 0.0001 in the 16-foot tunnel tests.

Figure 12 presents the drag polar at a Mach number of 0.775, which corresponds to the approximate cruise Mach number. The Reynolds number was 3.5×10^6 per foot. Again note that the drag scale does not start at zero. The agreement is seen to be satisfactory, the scatter in the data being no greater than about 4 counts of drag, or 1 percent, near the cruise lift. Figure 13 shows the variation of drag with Mach number at a constant lift coefficient of 0.48. The maximum spread between the curves is about 10 counts of drag, or 3 percent.

Comparison of Drag Results From Wind-Tunnel and Rocket-Technique Tests

The next logical question to be asked is: How well does the drag of a model measured in the wind tunnel correlate with the drag of the same model measured in free flight where the wind-tunnel constraints, such as boundary-reflected disturbances, are not present? Figure 14 shows a comparison of the drag coefficients of a four-engine delta-wing configuration from measurements in free flight by the rocket technique and in the Langley 16-foot transonic tunnel. The rocket and wind-tunnel models were identical as regards scale, surface smoothness, and so forth, and the Reynolds numbers for the two sets of data were about 4.0×10^6 per foot. In both cases, air flowed through the nacelles, and the drag data have been corrected for internal drag and base drag. Note the correlation which has been obtained between the rocket and wind-tunnel drag measurements. These investigations were made approximately 10 years ago. Although the rocket data extend to higher supersonic values than indicated, the Mach number capability of the tunnel at that time was limited to a maximum of about 1.12. The wind-tunnel data for Mach numbers of 1.05 and 1.12 shown by the solid symbols were affected by wind-tunnel boundary-reflected disturbances. These affected test points are included in the figure to illustrate further the problems of boundary-reflected disturbances which were discussed earlier.

Comparisons at Supersonic Speeds

The next correlation is for tests conducted at supersonic speeds. The requirements regarding the techniques for testing at supersonic speeds are not nearly as stringent as those for transonic testing. For example, the requirements for the sting-support system can be relaxed; and the chief consideration is to determine the model scale so that the model lies well within the Mach rhombus throughout the supersonic speed range. Experience has shown that it

is somewhat more difficult to achieve a turbulent boundary layer on models at supersonic speeds because of the thicker and more stable boundary layer present on the models. In the correlations which follow, however, transition was fixed on the models by using proper grit-type boundary-layer transition strips in a manner which assured turbulent conditions over the model surfaces.

Figure 15 shows the lift-drag polar for a delta-wing configuration at a Mach number of 3.0. This model is the same one that was used to obtain the transonic data presented in figures 10 and 11. Figure 16 shows the lift-drag polar for an arrow-wing configuration, also at a Mach number of 3.0; this configuration was investigated without nacelles and vertical tails. The tests of both configurations were made in the Langley Unitary Plan wind tunnel and in the Ames 8- by 7-foot supersonic wind tunnel at a constant Reynolds number of 3.0×10^6 per foot. Good correlation obviously has been achieved. The maximum scatter of the test points from the faired line amounts to 2 counts of drag, or less than 2 percent.

CONCLUDING REMARKS

Numerous comparisons have shown that drag data obtained for the same model in different wind tunnels at subsonic, transonic, and supersonic speeds agreed within 3 percent, provided the tests were made in accordance with the rules and techniques developed for wind-tunnel tests at these speeds. In the application of these rules and techniques, proper consideration must be given to model support systems, transition strips, tunnel wall effects, test limitations, and so forth. It has been further demonstrated that large-scale models, which permit high values of model Reynolds numbers, can be tested at subsonic speeds in relatively small transonic tunnels, and a high level of confidence can be placed in the results of such tests. It has also been shown that good correlation exists between model data obtained in the wind tunnel and by the rocket technique where the tunnel constraints are not present.

REFERENCES

1. Wright, Ray H.; Ritchie, Virgil S.; and Pearson, Albin O.: Characteristics of the Langley 8-Foot Transonic Tunnel With Slotted Test Section. NACA Rept. 1389, 1958. (Supersedes NACA RM L51H10 by Wright and Ritchie and RM L51K14 by Ritchie and Pearson.)

2. Ritchie, Virgil S.: Effects of Certain Flow Nonuniformities on Lift, Drag, and Pitching Moment for a Transonic-Airplane Model Investigated at a Mach Number of 1.2 in a Nozzle of Circular Cross Section. NACA RM L9E20a, 1949.

3. Hart, Roger G.: Effects of Stabilizing Fins and a Rear-Support Sting on the Base Pressures of a Body of Revolution in Free Flight at Mach Numbers From 0.7 to 1.3. NACA RM L52E06, 1952.

4. Love, Eugene S.: A Summary of Information on Support Interference at Transonic and Supersonic Speeds. NACA RM L53K12, 1954.

5. Tunnell, Phillips J.: An Investigation of Sting-Support Interference on Base Pressure and Forebody Chord Force at Mach Numbers From 0.60 to 1.30. NACA RM A54K16a, 1955.

6. Lee, George; and Summers, James L.: Effects of Sting-Support Interference on the Drag of an Ogive-Cylinder Body With and Without a Boattail at 0.6 to 1.4 Mach Number. NACA RM A57I09, 1957.

7. Cahn, Maurice S.: An Experimental Investigation of Sting-Support Effects on Drag and a Comparison With Jet Effects at Transonic Speeds. NACA Rept. 1353, 1958. (Supersedes NACA RM L56F18a.)

8. Mugler, John P., Jr.: Transonic Wind-Tunnel Investigation of the Static Longitudinal Aerodynamic Characteristics of Five Nose Cones Designed for Supersonic Impact. NASA TM X-432, 1961.

9. Braslow, Albert L.; and Knox, Eugene C.: Simplified Method for Determination of Critical Height of Distributed Roughness Particles for Boundary-Layer Transition at Mach Numbers From 0 to 5. NACA TN 4363, 1958.

10. Luoma, Arvo A.: Longitudinal Aerodynamic Characteristics at Transonic Speeds of a V/STOL Airplane Configuration With a Fixed Delta Wing Having Auxiliary Variable-Sweep Outboard Panels. NASA TM X-661, 1961.

11. Wright, Ray H.; and Barger, Raymond L.: Wind-Tunnel Lift Interference on Sweptback Wings in Rectangular Test Sections With Slotted Top and Bottom Walls. NASA Rept. R-241, 1966.

SHOCK-REFLECTION DISTANCE

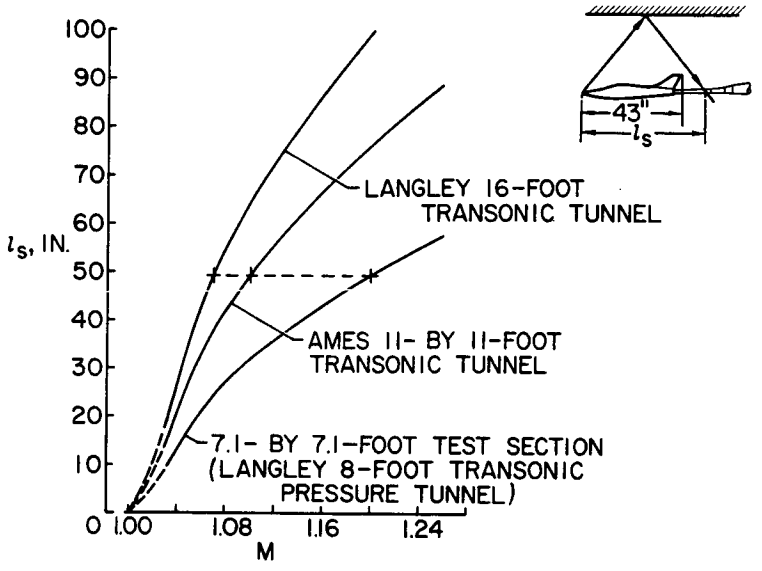

Figure 1

BOUNDARY-REFLECTED DISTURBANCES

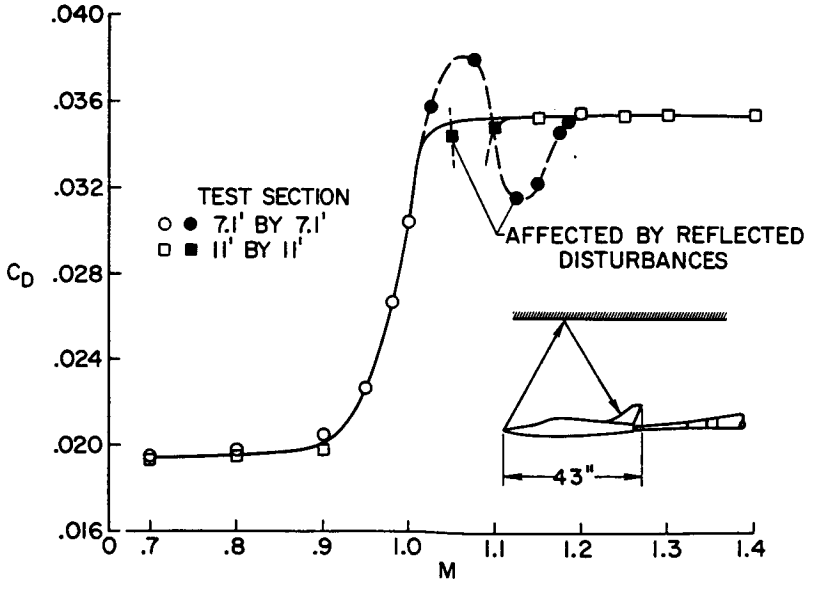

Figure 2

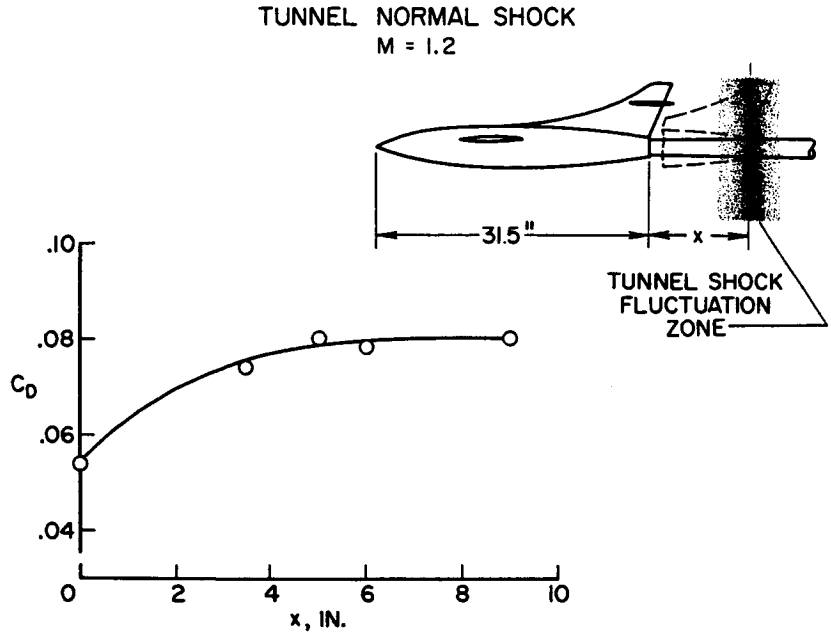

Figure 3

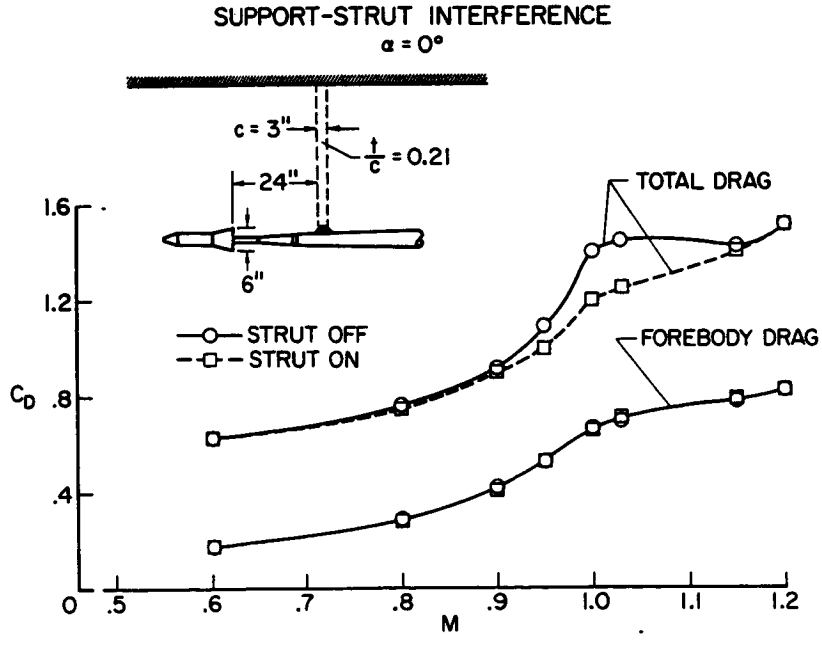

Figure 4

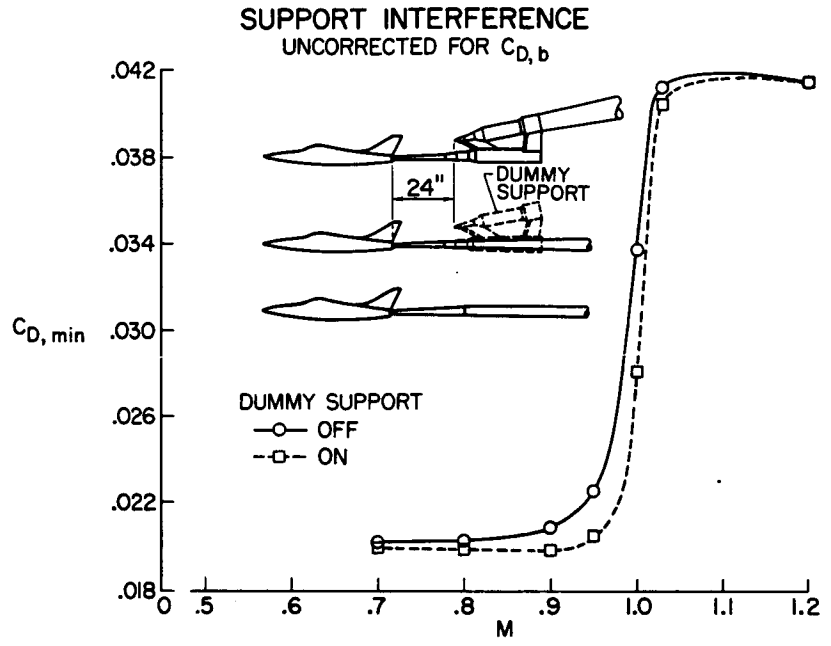

Figure 5

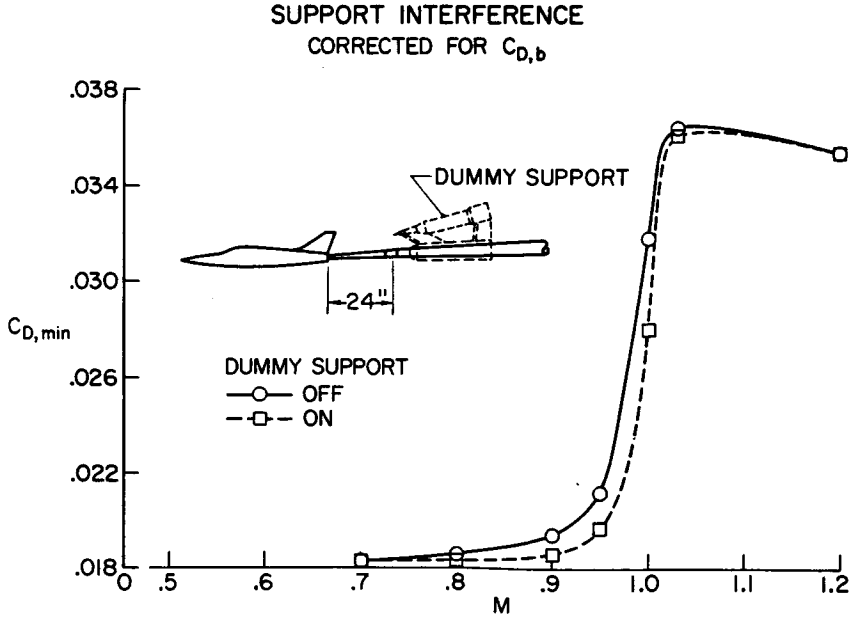

Figure 6

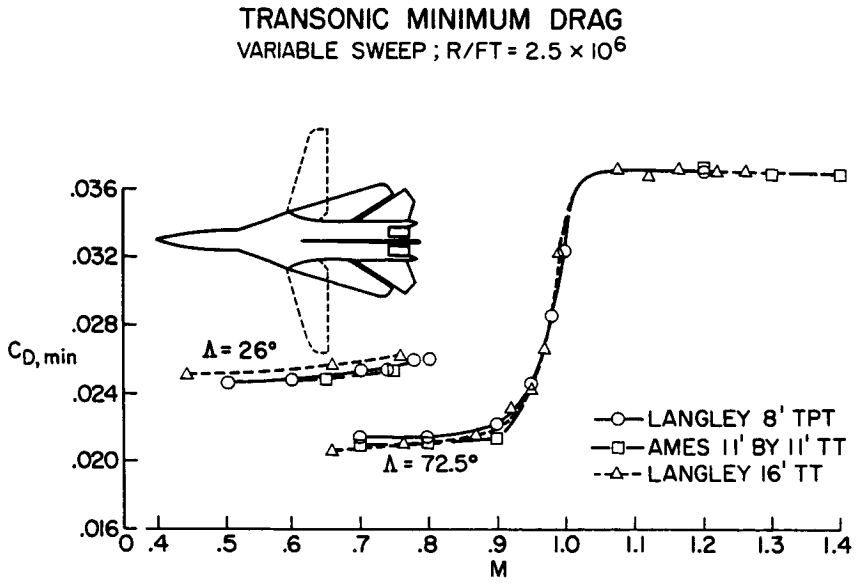

Figure 7

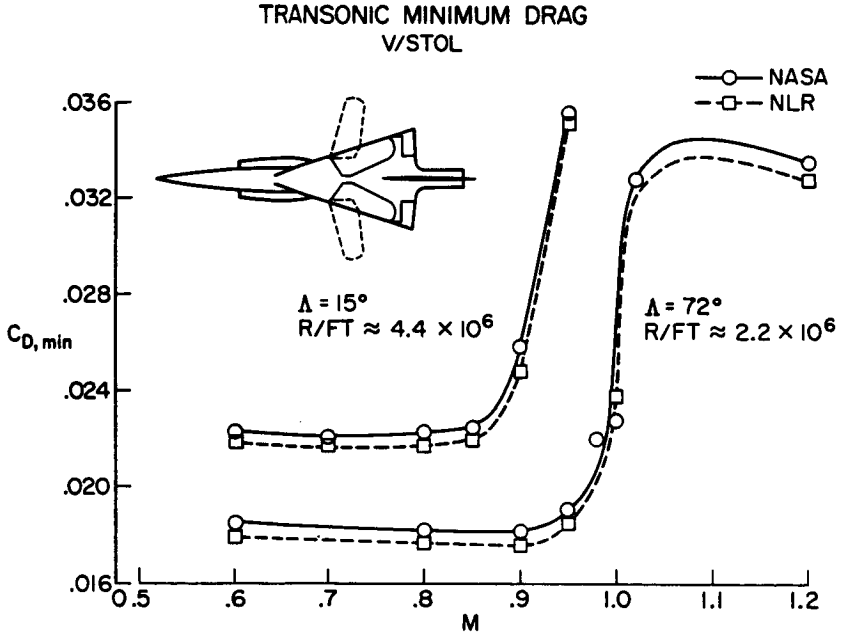

Figure 8

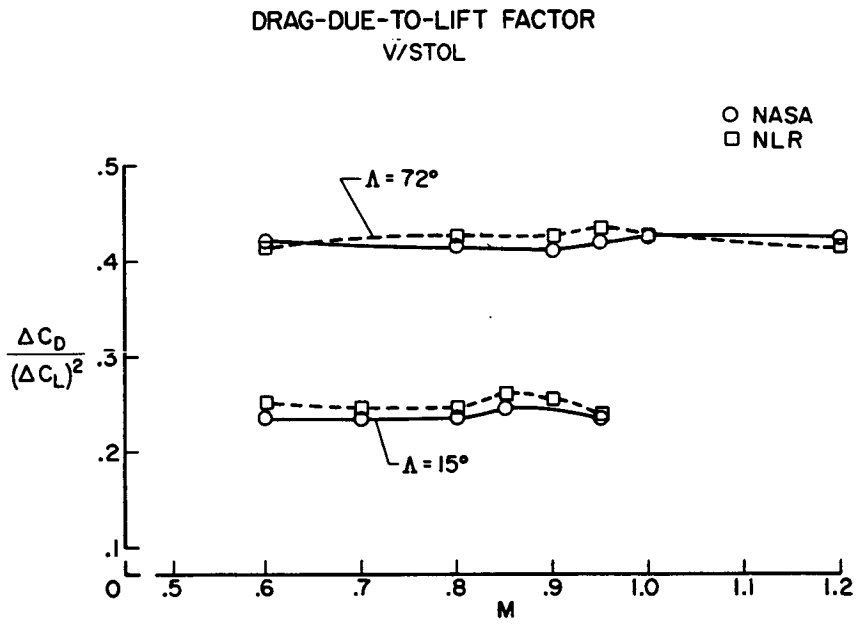

Figure 9

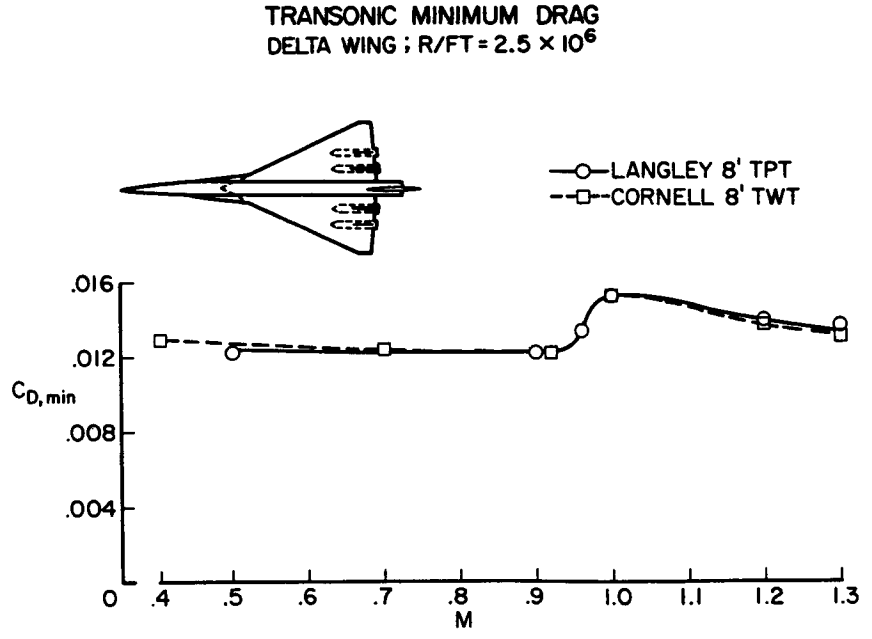

Figure 10

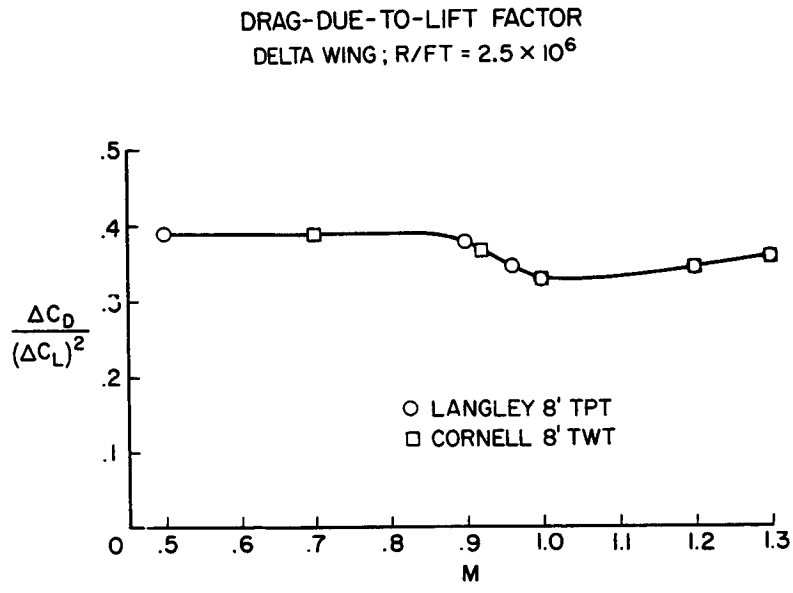

Figure 11

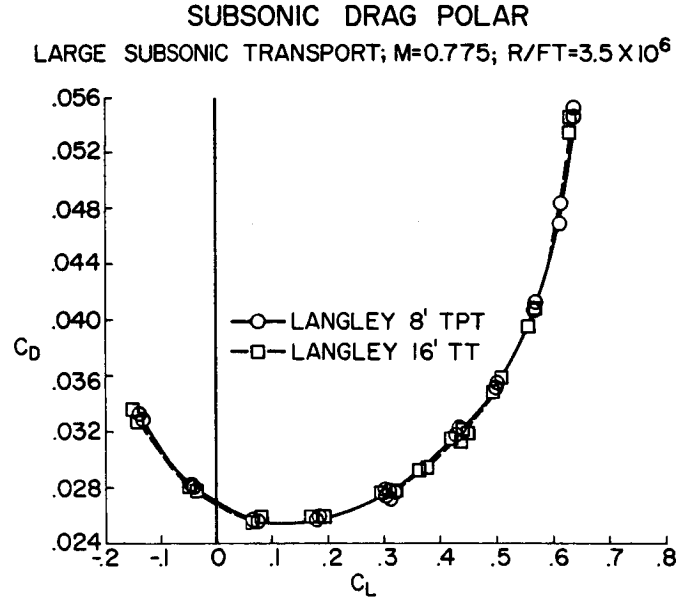

Figure 12

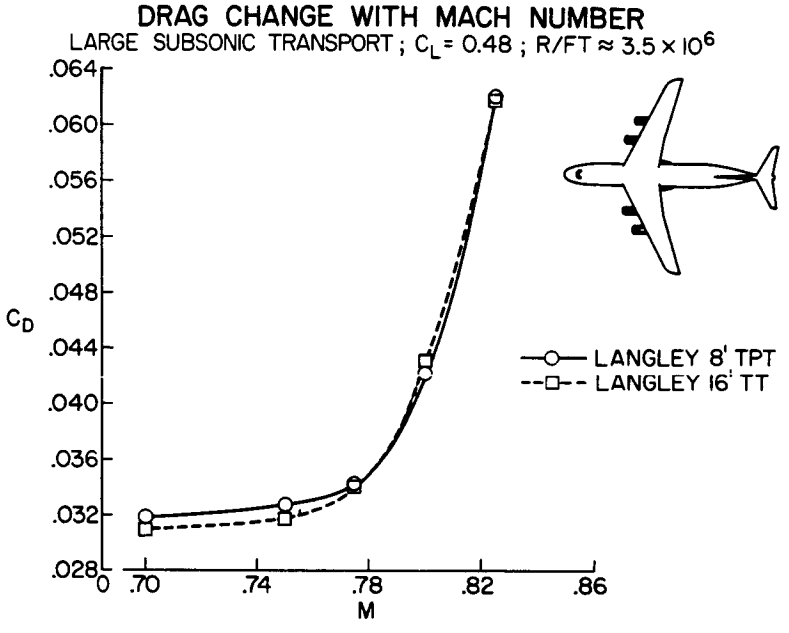

Figure 13

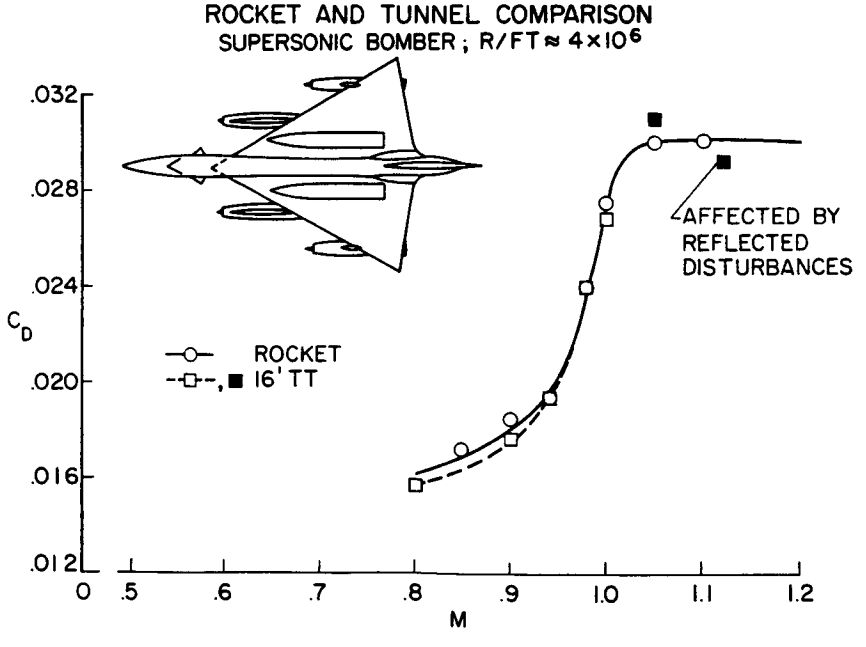

Figure 14

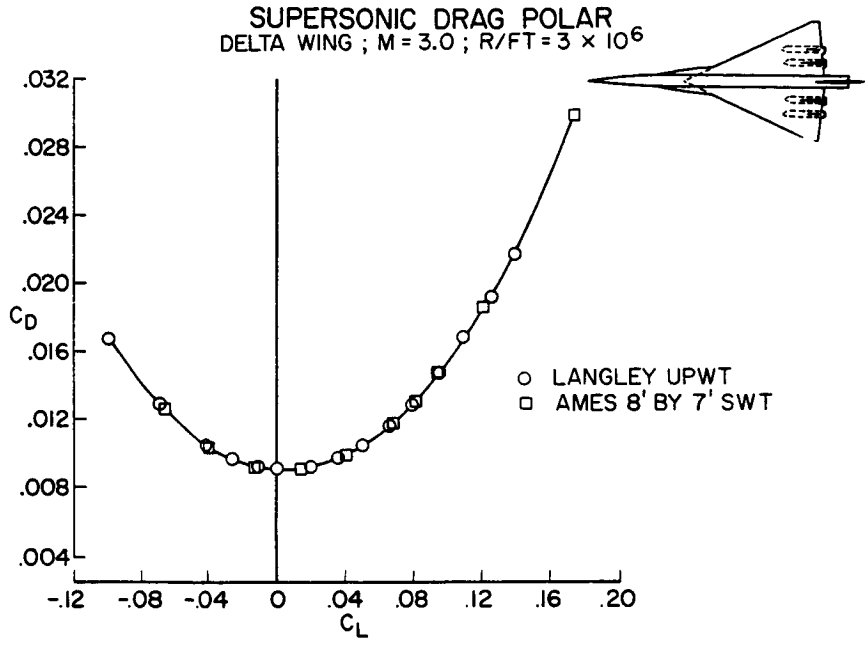

Figure 15

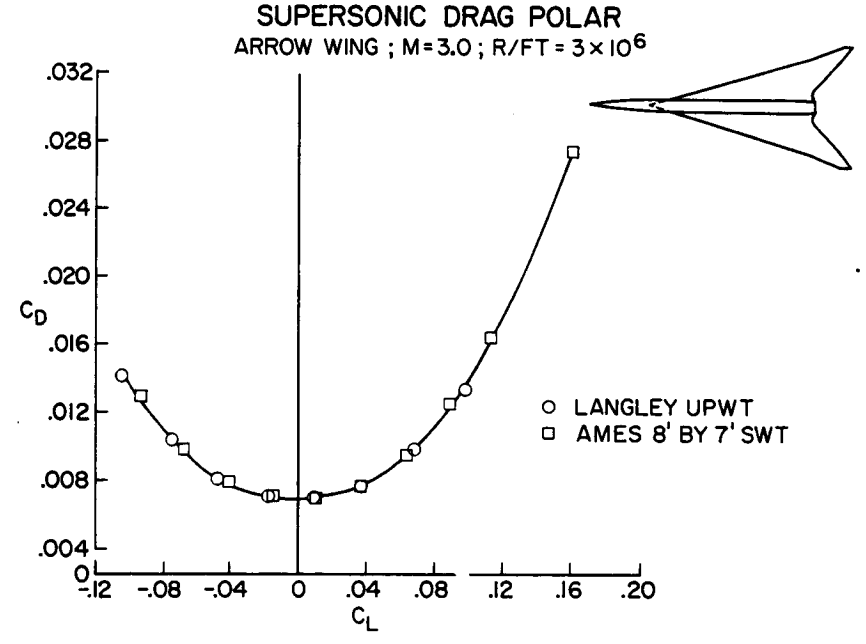

Figure 16